Mater Renew Sustain Energy (2016) 5:20
DOI 10.1007/s40243-016-0084-y

ORIGINAL PAPER

The synergistic effect of catalysts on hydrogen desorption properties of MgH_2–TiO_2–NiO nanocomposite

Farshad Rajabpour[1] · **Sharham Raygan**[1] · **Hossein Abdizadeh**[1]

Received: 1 August 2016 / Accepted: 19 October 2016 / Published online: 26 October 2016

Abstract The high desorption temperature and slow desorption kinetics of MgH_2 makes it less competitive for future mobile applications; using a catalyst accompanied by mechanical milling seems to be a good solution to overcome those problems. Therefore, the addition of TiO_2 and NiO to MgH_2 accompanied by 15 h of mechanical milling was considered in this study. The phase constituent and hydrogen desorption of the powder mixture were investigated using X-ray diffraction (XRD) and a Sievert-type apparatus, respectively. XRD results showed that after milling, no binary or ternary compounds were formed, but hydrogen desorption time decreased and the desorbed hydrogen content increased. It seems that the increase in desorbed hydrogen was related to the simultaneous catalytic effect of TiO_2 and NiO as well as mechanical milling. The results showed that the addition of both catalysts can improve the hydrogen desorption behavior of MgH_2-based nanocomposite compared to the addition of only one catalyst of the same amount.

Keywords MgH_2 · Hydrogen desorption · NiO · TiO_2 · Synergism

✉ Farshad Rajabpour
frajabpoor@gmail.com

[1] School of Metallurgy and Materials Engineering, College of Engineering, University of Tehran, Tehran, Iran

Introduction

Nowadays, it is a known fact that fossil fuels cause a series of ecological problems. Hydrogen is a viable energy resource alternative to conventional fossil fuels because it is clean and renewable and contains a high energy density. Hydrogen storage in metals (such as Mg and La) has numerous attractions such as high capacity, low cost, light weight and natural abundance. Mg and Mg-based materials are known to be suitable for solid-state hydrogen storage. Mg is light, abundant and forms MgH_2, which has a high storage capacity (7.6 wt%) and an acceptable cost of production [1]. Yet, MgH_2 is thermodynamically stable ($\Delta H = -74.5$ kJ mol^{-1}) and its hydrogen desorption is poor, below 350 °C [2]. The destabilization of MgH_2 can be performed by decreasing the particle size of the material, preferably down to the nanoscale, and addition of catalysts [3–5]. Decreasing the particle size can result in more free surface and, therefore, better kinetics can result from short diffusion pathways along grain boundaries.

Improvement of the storage behavior of MgH_2 has been investigated using several catalysts, including elemental [6–10], intermetallic [11–14], oxide [5, 15–18], halide [19–22], hydride [23–25] and other additives [26, 27]. Among the oxide catalysts, TiO_2 is known to be remarkable. Many investigations have been performed on the catalytic effect of TiO_2 on MgH_2 [5, 16, 27–29]. Wang et al. [30] milled a mixture of Mg and 10 wt% of TiO_2 for 6 h and claimed that TiO_2 particles provided a diffusion way for H atoms which improved the diffusion rate, and, consequently, the desorption of hydrogen. Polanski et al. [16] ball-milled MgH_2 with Cr_2O_3, Fe_3O_4, Fe_2O_3 and TiO_2 for 20 h. They reported that among all the oxide additives, TiO_2 showed the best kinetics in desorption. Gattia et al.

[31] ball milled MgH_2 with 5 wt% of TiO_2 and then added expanded natural graphite. They stated that the kinetics was improved and a good cyclability was also observed. Also, it has been proved that TiO_2 has a better catalytic effect in the form of anatase compared to rutile [32]. The effect of elemental nickel on MgH_2 [4, 7, 9, 33] and the hydrogen storage properties of Mg + NiO and MgH_2 + -NiO mixtures have also been studied [34, 35]; however, to the best of our knowledge, the catalytic effect of NiO + TiO_2 on MgH_2 has not yet been investigated. It has been reported that the presence of two oxide catalysts can improve the hydrogen storage properties of MgH_2 compared to one oxide catalyst [36]. In this study, we investigated the hydrogen desorption properties of MgH_2–TiO_2–NiO, as well as MgH_2–TiO_2 and MgH_2–NiO nanocomposites. In this regard, the phase constituent of the powder mixture after ball milling, morphology, size and distribution of the particles, and the hydrogen storage properties of the samples were studied.

The experiment

Material preparation

MgH_2 (Alfa Aesar, <140 μm, purity: 98%), TiO_2 (Merck, <0.2 μm, purity: 99.5%) and NiO (Scharlau, Spain, <20 μm, purity: 99.9%) powders were used as raw materials. The powders were ball milled using high-energy planetary ball mill (Asia Sanat Rakhsh/2400) with a ball to powder ratio of 20:1 and a rotation speed of 250 RPM under a high-purity argon atmosphere for 15 h. For the milling process, a hardened Cr–steel vial accompanied by hardened bearing steel balls with 8-, 10- and 15-mm diameters were used. In all the samples, 5 wt% of catalyst was added to MgH_2. About 1 wt% of stearic acid (Alfa Aesar, purity: >99%) was used as a process control agent (PCA).

Material characterization

Phase composition analysis was performed using a Philips X'Pert Pro diffractometer with Cu kα ($\lambda = 0.1541874$ nm) radiation with a step size of 0.02° and X'Pert High Score Plus v2.2b (PANalytical Company). The mean crystallite size and the lattice micro strain of the particles were measured using the Williamson–Hall method [37]:

$$\beta_{\text{sample}}\cos\theta = K\lambda/\delta + 2\varepsilon\sin\theta, \quad (1)$$

where β_{sample} is the full width at half-maximum (FWHM) of the milled powder, θ the position of the peak maximum, K the Scherrer constant (about 0.9), λ the beam wavelength, δ the crystallite size, and ε the lattice micro strain introduced by ball milling. For instrumental correction, the Gaussian relationship was used [38]:

$$\beta_{\text{sample}} = \sqrt{\beta^2_{\text{experimental}} - \beta^2_{\text{instrumental}}} \quad (2)$$

where $\beta_{\text{experimental}}$ is the measured FWHM of the annealed nickel powders.

Hydrogen desorption results were obtained and studied using a handmade Sievert apparatus. The activation of samples in the Sievert method was performed at 190 °C under 4-bar pressure of highly pure hydrogen gas (with the purity of 99.99 wt%).

The field emission scanning electron microscope (FESEM) Sigma (Zeiss Company) and the scanning electron microscope MV 2300 (Tescan Company) were used to observe the morphology and particle size of the powders. Image analysis was performed using MIP4 Student (Nahamin Pardazan Asia Company).

Results and discussion

Phase analysis

Figure 1 shows the X-ray diffraction (XRD) patterns of the samples after 15 h of ball milling. It can be observed from XRD patterns of ball-milled MgH_2 (BMM) that the peaks of β-MgH_2, which is known as low-pressure MgH_2, are broadened after milling. This indicates that the crystalline size has decreased and strain has been induced in the lattice. The diffraction pattern of the BMM sample shows one obvious MgO peak and one peak overlapping the MgH_2 peaks, which is in agreement with other studies [39]. The presence of MgO in the ball-milled samples is probably due to the high activity of Mg from 2% impurity in MgH_2. The peaks of metastable γ-MgH_2, which are not sharp but have been confirmed before [40], can be observed in the diffraction pattern. The formation of γ-MgH_2 was also reported for samples which had been milled for more than 10 h [41]. As shown in Table 1, the crystallite size has decreased and the lattice strain increased in the BMM sample compared to the unmilled MgH_2, indicating that more free active surface is available for recombination of hydrogen molecules as well as smaller diffusion pathway for hydrogen atoms.

The diffraction pattern of the sample with TiO_2 catalyst in the form of anatase (MT) shows the presence TiO_2, MgH_2 and MgO. The addition of hard oxide particles to the non-ductile MgH_2 helped decrease the crystallite size and introduce more strain to the lattice [42]. During the process of ball milling, the continuous fracture and micro-welding goes on up to the steady state [43]. Thus, as shown in Table 1, the addition of hard particle can help break up

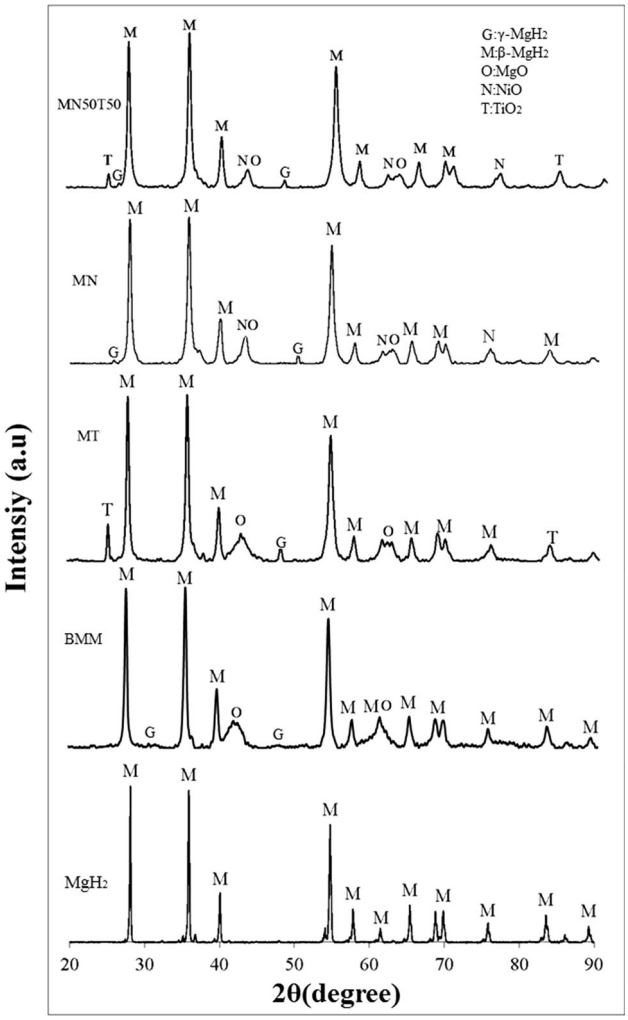

Fig. 1 XRD patterns of the different samples

Table 1 Mean crystallite size and lattice strain of the ball-milled powders

Sample name	Mean crystallite size (nm)	Lattice strain (%)
MgH_2	45	0
BMM	38	0.11
MT	25	0.16
MN	28	0.14
MN50T50	27	0.15

MgH_2 particles and result in decreasing of the crystallite size and increasing of lattice strain and active surface area [44]. The sample with NiO catalyst (MN) shows the presence of NiO and MgH_2 and overlapped MgO peaks at 43° and 62°. Due to the hard nature of the oxides, they can be used as a particle refinement agent; therefore, as shown in Table 1, this sample shows reduced crystallite size and increased lattice strain. All the raw materials were present in the XRD pattern of the sample with 5 wt% of catalyst containing a mixture of 50 wt% of TiO_2 and 50 wt% of NiO (MN50T50). This sample contained two types of oxidic catalysts and, as a result, its crystallite size decreased compared to that of the BMM sample, and its lattice strain increased. No new binary or ternary components were formed in any of the catalyst-containing samples.

It is clear that the differences between the mean crystallite size and lattice strain of all three catalyzed samples are negligible. This could be due to the equality of the sample preparation process, ball mill time and ball to powder ratio for all the samples.

Morphology of the powders

Figure 2 shows the FESEM images of the (a) as-received MgH_2, (b) BMM, (c) MN, (d) MT and (e) MN50T50 samples. The results of image analysis of different FESEM images of the samples are shown in Fig. 3. The particle size of the mixture has significantly reduced after 15 h of ball milling, as shown in Figs. 2b and 3a for the BMM sample. It is obvious that mechanical milling is effective in decreasing the size of particles and providing more fresh active surface. It has been reported that the kinetics of MgH_2 can be enhanced by decreasing the particle size, which can lead to a reduction in the hydrogen diffusion pathway [45]. It seems that the highest cumulative value for the distribution of particle size in all samples is between 80 and 250 nm, and the cumulative value for larger particles is negligible. The inhomogeneous contact of the powders and steel balls during the ball-milling process could be the cause of this inhomogeneous particle size distribution [46]. It can be observed that the addition of catalyst to the MgH_2 and 15 h of ball milling reduce the particle size, which can have the benefit of more free surface and probably result in increased hydrogen desorption [38]. As shown in Fig. 3, the emergence of smaller particles in the catalyzed sample can confirm that the presence of hard oxide particles in the non-ductile MgH_2 can result in a smaller particle size and, consequently, a better hydrogen desorption behavior. The emergence of nano-sized particles in the sample shows that high-energy ball milling is an ideal method to decrease the particle size of the powder particles down to the nano-scale and, consequently, increase the surface area and potential sites of hydrogen desorption.

Figure 4 shows the results of EDS analysis for the MN50T50 sample. It can be seen that the distributions of TiO_2 and NiO on the surface of MgH_2 are uniform and approximately the same.

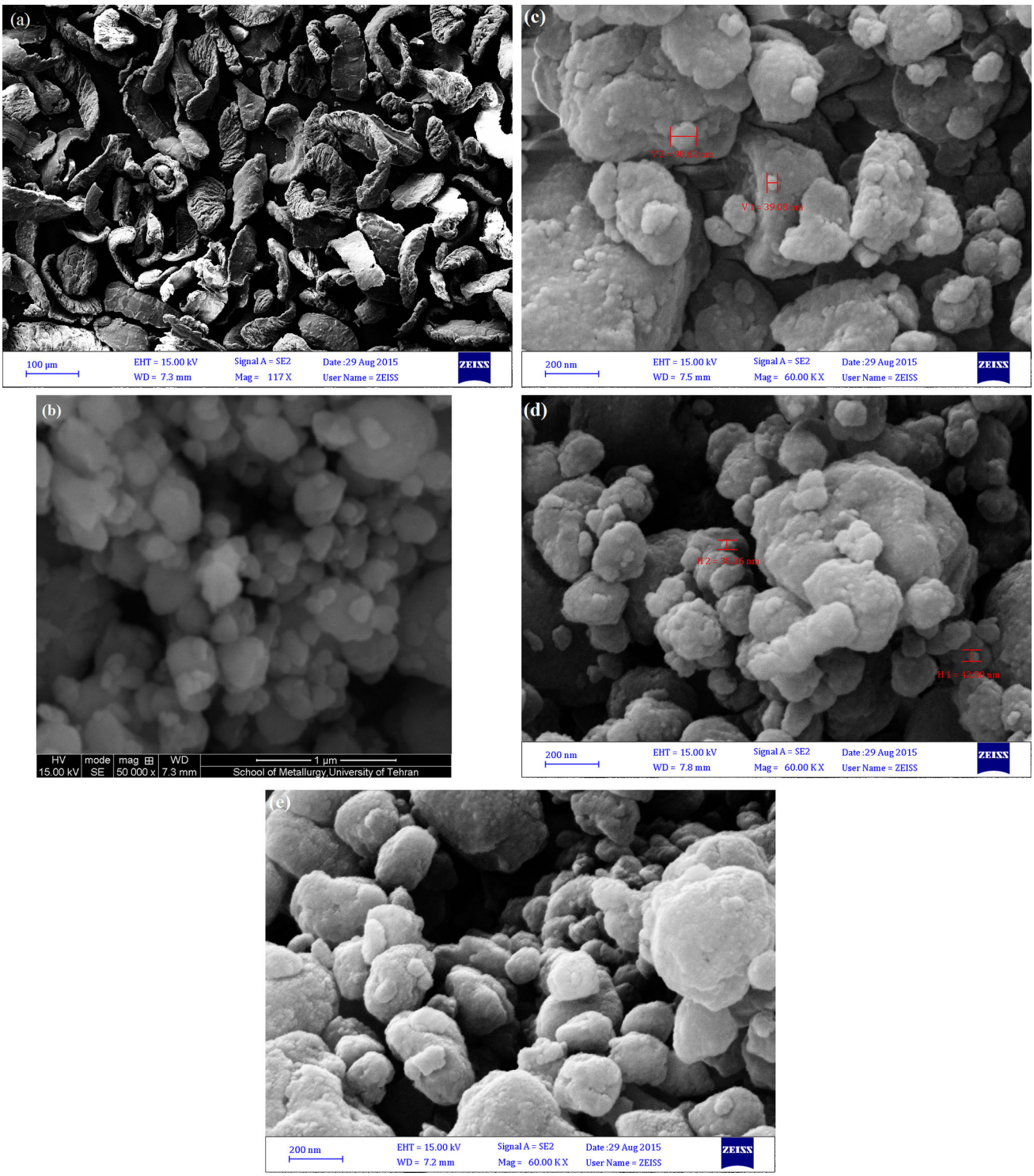

Fig. 2 FESEM images of **a** as-received MgH_2, **b** BMM, **c** MN, **d** MT and **e** MN50T50 samples

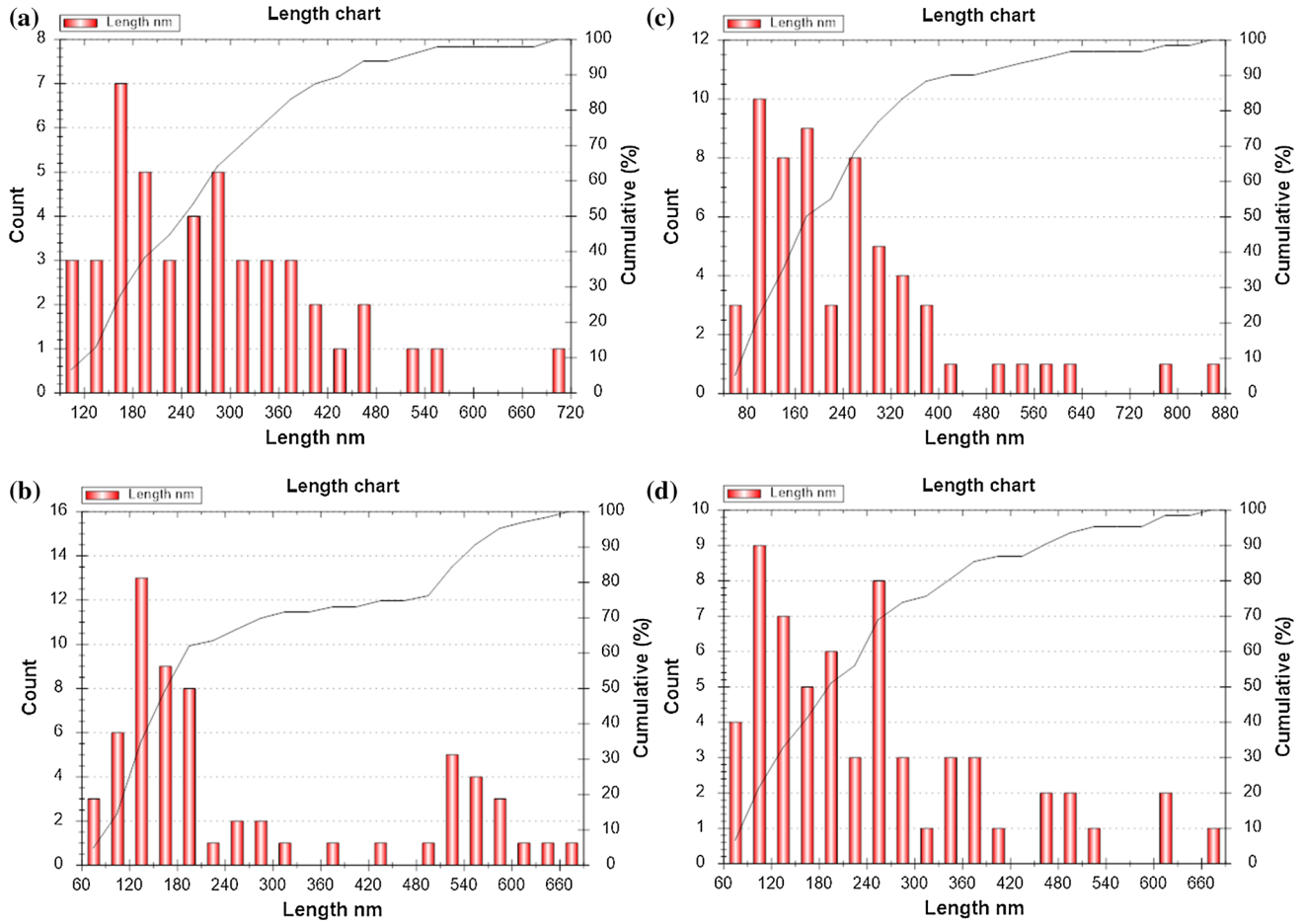

Fig. 3 Results of image analysis of the SEM images of **a** BMM, **b** MN, **c** MT and **d** MN50T50 samples

Hydrogen desorption properties

MgH_2 and BMM samples

Figure 5 shows the hydrogen desorption results of the as-received MgH_2, BMM, MT, MN and MN50T50 samples, obtained from the Sievert apparatus at 350 °C. The desorption rate of the samples in the first 200 s of the desorption process is shown in Fig. 6. Moreover, Fig. 7 demonstrates the onset time of desorption for various samples. It should be mentioned that the threshold of hydrogen desorption onset time has been considered to be after 0.5 wt% of hydrogen desorption. While MgH_2 desorbed nothing after 2500 s, the BMM sample desorbed 1.10 wt% of hydrogen starting after 642 s with a slow rate within the first 200 s, as shown in Figs. 6 and 7, which is in good agreement with previous studies [47, 48]. For example, Chitsazkhoyi et al. [47] claimed that after 30 h of ball milling, pure MgH_2 released about 1 wt% of hydrogen. In that research, all the samples which had been ball milled for less than 30 h, released less than 1 wt% of hydrogen. It has been claimed that increasing the hydrogen desorption of ball-milled MgH_2 could be due to the (1) refinement of the powder particles, (2) higher specific surface area which can lead to more active sites for gas–solid reaction, (3) decreasing of the pathways for the diffusion of hydrogen through nanometric grains and (4) the lattice strain which was introduced to the system and can affect the diffusion and thus the decomposition rate [36]. In addition, the presence of metastable γ-MgH_2 can affect the desorption process. Since the γ-MgH_2 has a lower desorption enthalpy, its presence in the mixture can help the desorption kinetics [41]. It has been proposed that the rate-limiting step for hydrogen desorption is either the diffusion pathway of hydrogen through the grains to the surface or the recombination of hydrogen molecules on the surface of the particles [42]. In both theories, particle size decrease can enhance the desorption kinetics. Mechanical milling can reduce the diffusion pathways by decreasing the particle size, which can also increase the active surface area for the recombination of hydrogen molecules.

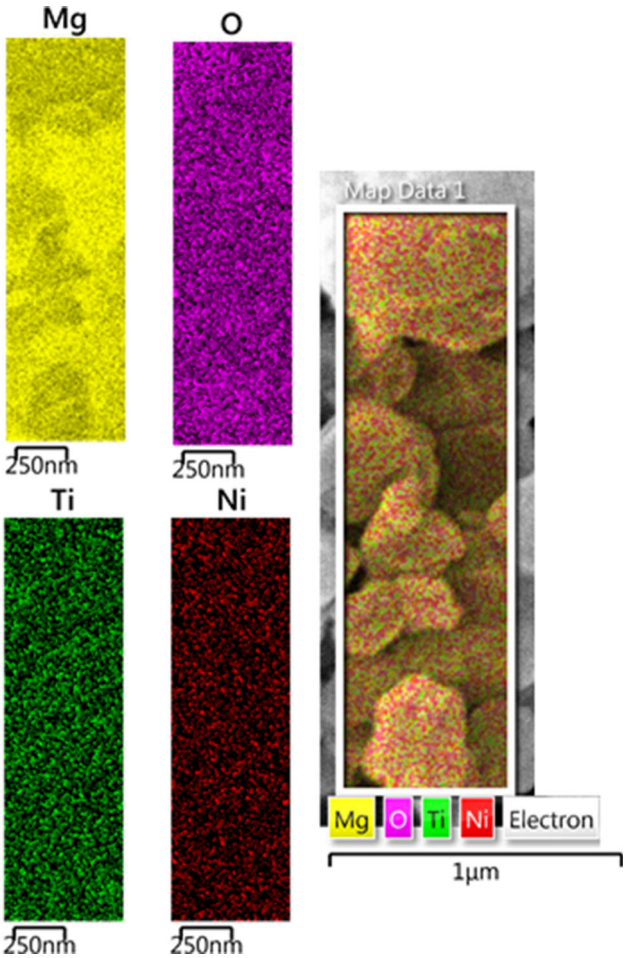

Fig. 4 EDS analysis of the MN50T50 sample

The effect of NiO

According to previous studies, the addition of catalysts can enhance kinetics using the spillover mechanism by allowing electron transfer and hydrogen dissociation/recombination on the surface of the catalyst [49]. With the addition of NiO, the desorption process starts after 119 s, and the desorption rate is higher than that of the BMM and MN50T50 samples within the first 200 s. Desorption of hydrogen accedes to a steady state after about 900 s and no more hydrogen is desorbed. The mixture in the presence of NiO desorbs 2.94 wt% at 350 °C. This result is in agreement with those of previous studies [34]. As it was discussed before, the decreasing of the onset time compared to the non-catalyzed MgH_2 could be related to the presence of hard oxide particles which can lead to a smaller crystallite size and more lattice strain (Table 1), the spillover mechanism and the presence of γ-MgH_2.

The effect of TiO_2

The addition of TiO_2 enhanced the desorption behavior of MgH_2. The MT sample desorbed 1.97 wt%. The desorption starts after 59 s at 350 °C, which is the fastest of all samples, and continues with a moderate rate within the first 200 s. Hydrogen desorption from the MT sample was in a steady state after about 1000 s. The amount of hydrogen desorbed from the MT sample is in agreement with those reported in previous studies. For instance, Wang et al. [50] reported that the sample which had been milled with TiO_2 for 10 h

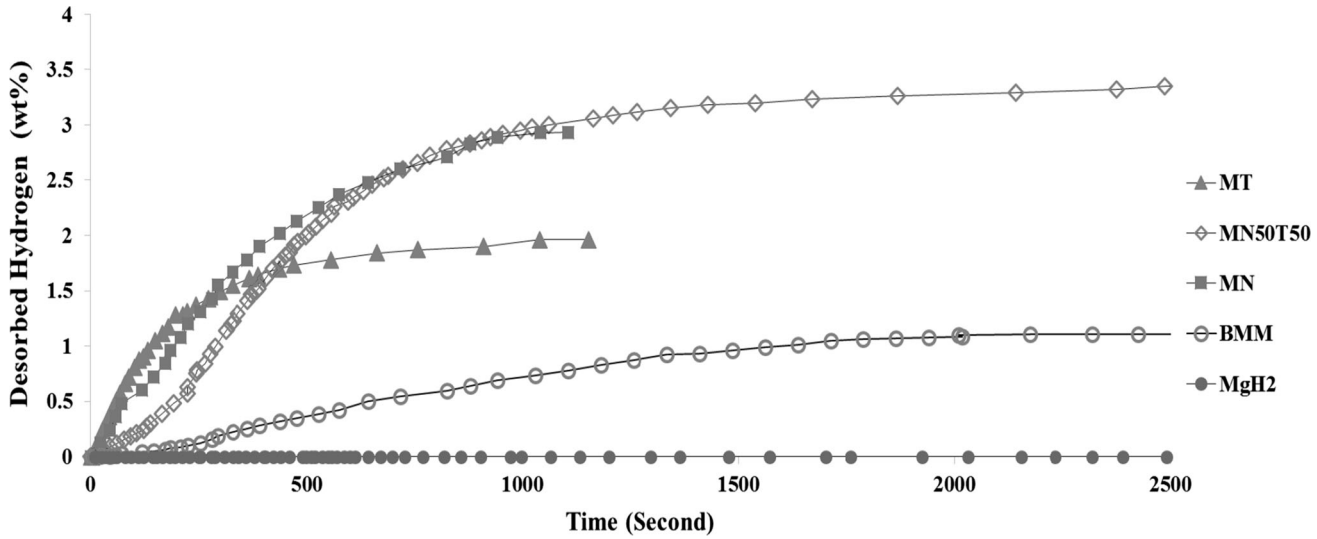

Fig. 5 Hydrogen desorption results of MgH_2, MT, MN and MN50T50 samples

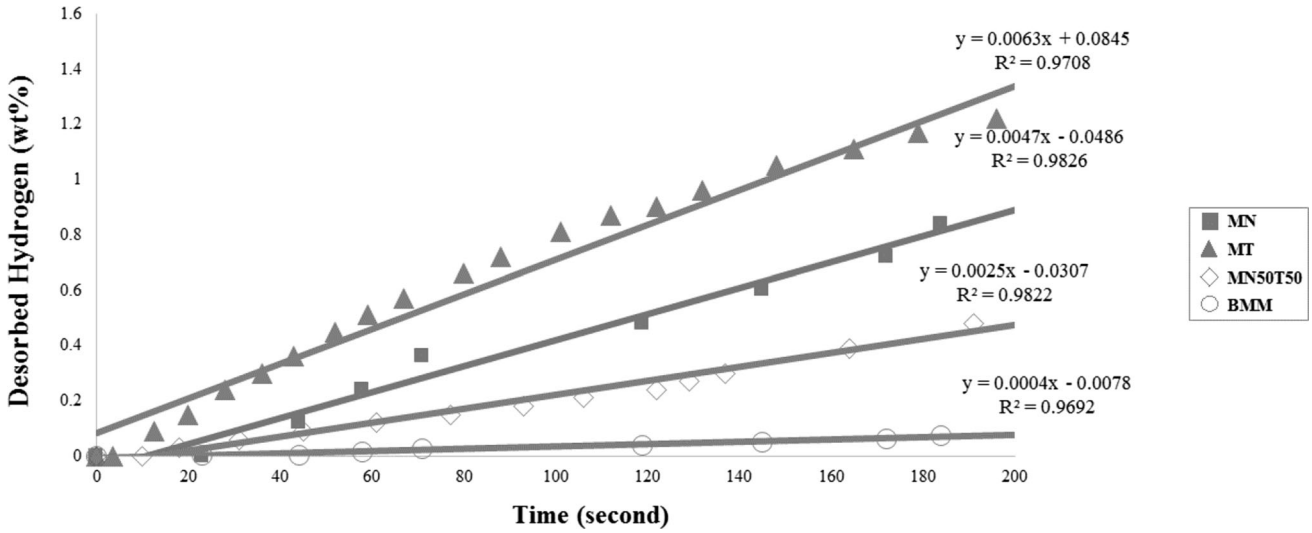

Fig. 6 Desorption results of the samples within the first 200 s

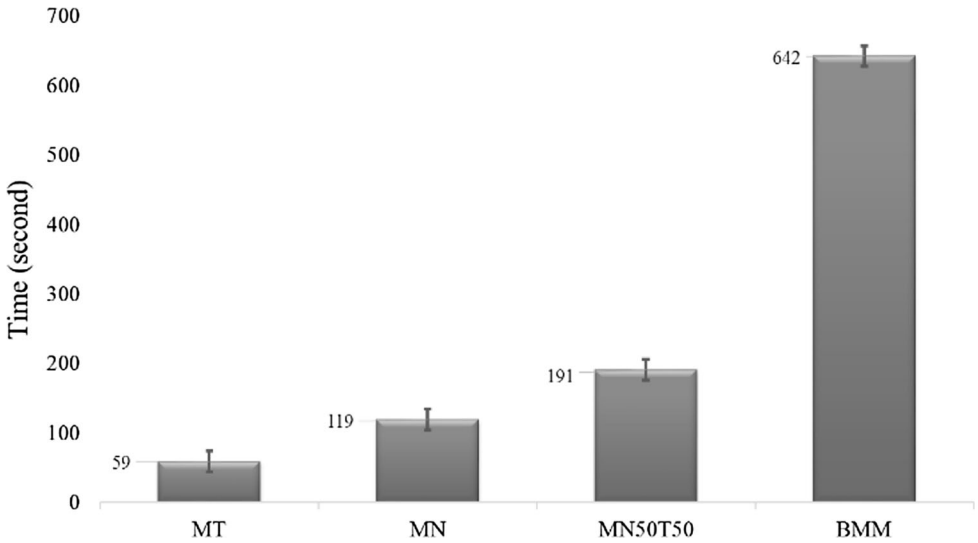

Fig. 7 Onset time of hydrogen desorption of the samples

released 1 wt% of hydrogen. It was proved that the low hydrogen desorption capacity of TiO_2-containing sample could be due to the formation of $TiH_{1.971}$ during the desorption process [51]. In addition to the abovementioned reasons, it was claimed that TiO_2 was reduced during the desorption process which resulted in active species responsible for the enhancement of hydrogen desorption [32].

Simultaneous effects of TiO_2 and NiO

The decomposition of MN50T50 led to the desorption of 3.35 wt% of hydrogen. This sample started hydrogen desorption after 191 s with a relatively low rate, but continued to desorb it up to 2500 s. It can be concluded that the difference between hydrogen desorption of MN50T50 and that of the other two catalyzed samples is related to the chemical composition of the mixture, since (1) the procedure of sample preparing and desorption test was the same for all the samples, (2) the crystallite size and the lattice strain differences of the catalyzed samples were negligible, (3) the XRD for none of the samples showed the existence of new binary or ternary compounds and (4) the elemental distributions of the catalysts were homogeneous and the same. It seems that the simultaneous presence of both catalysts resulted in a synergic effect, leading to a higher desorbed hydrogen content.

Conclusions

The hydrogen desorption of MgH_2 catalyzed with two different oxidic catalysts was investigated in the present study. It was proved that hydrogen desorption increased by mechanical milling and the addition of the catalysts, due to

the decrease of the particle size and increase of the active sites for hydrogen desorption, as well as the effect of catalysts. Ball-milled MgH_2 desorbed 1.1 wt% of hydrogen at 350 °C, while the unmilled MgH_2 desorbed nothing under the same condition. The addition of 5 wt% of TiO_2 increased the hydrogen desorption of the mixture and resulted in a 1.97 wt% desorption of hydrogen at 350 °C, which could be related to the catalytic effect of anatase as well as mechanical milling. In the presence of NiO, MgH_2 desorbed 2.94 wt% of hydrogen at 350 °C. In the simultaneous presence of NiO and TiO_2, the samples desorbed 3.35 wt% of hydrogen, which could be related to the synergic effect of TiO_2 and NiO catalysts. There was no evidence of new binary or ternary compounds in the X-ray results of the catalyst-containing samples; thus, the differences in hydrogen desorption could not be related to the formation of new compounds. Moreover, with decrease in the particle and crystallite size, the lattice strain increased in all of the samples; but the differences were not big enough to cause a significant difference in the amount of desorbed hydrogen. Thus, it seems that these differences are the result of synergism of catalysts.

Compliance with ethical standards

Conflict of interest The authors declare that they have no conflict of interest.

References

1. Chen, B.-H., Chuang, Y.-S.: Improving the hydrogenation properties of MgH_2 at room temperature by doping with nano-size ZrO_2 catalyst. J. Alloy. Compd. **655**, 21–27 (2016)
2. Maddalena, A., Petris, M., Palade, P., Sartori, S., Principi, G., Settimo, E., et al.: Study of Mg-based materials to be used in a functional solid state hydrogen reservoir for vehicular applications. Int. J. Hydrog. Energy **31**, 2097–2103 (2006)
3. Nielsen, T.K., Manickam, K., Hirscher, M., Besenbacher, F., Jensen, T.R.: Confinement of MgH_2 nanoclusters within nanoporous aerogel scaffold materials. ACS Nano **3**, 3521–3528 (2009)
4. Liang, G., Huot, J., Boily, S., Van Neste, A., Schulz, R.: Catalytic effect of transition metals on hydrogen sorption in nanocrystalline ball milled MgH_2–Tm (Tm = Ti, V, Mn, Fe and Ni) systems. J. Alloy. Compd. **292**, 247–252 (1999)
5. Oelerich, W., Klassen, T., Bormann, R.: Metal oxides as catalysts for improved hydrogen sorption in nanocrystalline Mg-based materials. J. Alloy. Compd. **315**, 237–242 (2001)
6. Varin, R., Li, S., Chiu, C., Guo, L., Morozova, O., Khomenko, T., et al.: Nanocrystalline and non-crystalline hydrides synthesized by controlled reactive mechanical alloying/milling of Mg and Mg–X (X = Fe Co, Mn, B) systems. J. Alloy. Compd. **404**, 494–498 (2005)
7. Bobet, J., Akiba, E., Nakamura, Y., Darriet, B.: Study of Mg-M (M = Co, Ni and Fe) mixture elaborated by reactive mechanical alloying—Hydrogen sorption properties. Int. J. Hydrog. Energy **25**, 987–996 (2000)
8. Denis, A., Sellier, E., Aymonier, C., Bobet, J.-L.: Hydrogen sorption properties of magnesium particles decorated with metallic nanoparticles as catalyst. J. Alloy. Compd. **476**, 152–159 (2009)
9. Bobet, J.-L., Chevalier, B., Song, M.-Y., Darriet, B., Etourneau, J.: Reactive mechanical grinding of magnesium in hydrogen and the effects of additives. Mater. Manuf. Process. **17**, 351–361 (2002)
10. Jeon, K.-J., Theodore, A., Wu, C.-Y., Cai, M.: Hydrogen absorption/desorption kinetics of magnesium nano-nickel composites synthesized by dry particle coating technique. Int. J. Hydrog. Energy **32**, 1860–1868 (2007)
11. Sabitu, S., Gallo, G., Goudy, A.: Effect of TiH_2 and Mg_2Ni additives on the hydrogen storage properties of magnesium hydride. J. Alloy. Compd. **499**, 35–38 (2010)
12. Yu, X., Yang, Z., Liu, H., Grant, D., Walker, G.S.: The effect of a Ti-V-based BCC alloy as a catalyst on the hydrogen storage properties of MgH_2. Int. J. Hydrog. Energy **35**, 6338–6344 (2010)
13. Pighin, S., Capurso, G., Russo, S.L., Peretti, H.: Hydrogen sorption kinetics of magnesium hydride enhanced by the addition of Zr_8 Ni_{21} alloy. J. Alloy. Compd. **530**, 111–115 (2012)
14. Laversenne, L., Andrieux, J., Plante, D., Lyard, L., Miraglia, S.: In operando study of TiVCr additive in MgH_2 composites. Int. J. Hydrog. Energy **38**, 11937–11945 (2013)
15. Song, M., Bobet, J.-L., Darriet, B.: Improvement in hydrogen sorption properties of Mg by reactive mechanical grinding with Cr 2 O 3, Al 2 O 3 and CeO 2. J. Alloy. Compd. **340**, 256–262 (2002)
16. Polanski, M., Bystrzycki, J.: Comparative studies of the influence of different nano-sized metal oxides on the hydrogen sorption properties of magnesium hydride. J. Alloy. Compd. **486**, 697–701 (2009)
17. Borgschulte, A., Bösenberg, U., Barkhordarian, G., Dornheim, M., Bormann, R.: Enhanced hydrogen sorption kinetics of magnesium by destabilized $MgH_2 - \delta$. Catal. Today **120**, 262–269 (2007)
18. Milošević, S., Rašković-Lovre, Ž., Kurko, S., Vujasin, R., Cvjetićanin, N., Matović, L., et al.: Influence of VO 2 nanostructured ceramics on hydrogen desorption properties from magnesium hydride. Ceram. Int. **39**, 51–56 (2013)
19. Ivanov, E., Konstanchuk, I., Bokhonov, B., Boldyrev, V.: Hydrogen interaction with mechanically alloyed magnesium–salt composite materials. J. Alloy. Compd. **359**, 320–325 (2003)
20. Jin, S.-A., Shim, J.-H., Cho, Y.W., Yi, K.-W.: Dehydrogenation and hydrogenation characteristics of MgH_2 with transition metal fluorides. J. Power Sourc. **172**, 859–862 (2007)
21. Deledda, S., Borissova, A., Poinsignon, C., Botta, W., Dornheim, M., Klassen, T.: H-sorption in MgH_2 nanocomposites containing Fe or Ni with fluorine. J. Alloy. Compd. **404**, 409–412 (2005)
22. Malka, I., Bystrzycki, J., Płociński, T., Czujko, T.: Microstructure and hydrogen storage capacity of magnesium hydride with zirconium and niobium fluoride additives after cyclic loading. J. Alloy. Compd. **509**, S616–S620 (2011)
23. Lu, J., Choi, Y.J., Fang, Z.Z., Sohn, H.Y., Rönnebro, E.: Hydrogen storage properties of nanosized $MgH_2 - 0.1$ TiH_2 prepared by ultrahigh-energy − high-pressure milling. J. Am. Chem. Soc. **131**, 15843–15852 (2009)
24. Yavari, A., De Castro, J., Vaughan, G., Heunen, G.: Structural evolution and metastable phase detection in MgH_2–5% NbH

nanocomposite during in situ H-desorption in a synchrotron beam. J. Alloy. Compd. **353**, 246–251 (2003)
25. Czujko, T., Varin, R., Wronski, Z., Zaranski, Z., Durejko, T.: Synthesis and hydrogen desorption properties of nanocomposite magnesium hydride with sodium borohydride ($MgH_2 + NaBH_4$). J. Alloy. Compd. **427**, 291–299 (2007)
26. Ranjbar, A., Guo, Z., Yu, X., Attard, D., Calka, A., Liu, H.: Effects of SiC nanoparticles with and without Ni on the hydrogen storage properties of MgH_2. Int. J. Hydrog. Energy **34**, 7263–7268 (2009)
27. Pitt, M.P., Paskevicius, M., Webb, C., Sheppard, D., Buckley, C., Gray, E.M.: The synthesis of nanoscopic Ti based alloys and their effects on the MgH_2 system compared with the $MgH_2 + 0.01$ Nb_2O_5 benchmark. Int. J. Hydrog. Energy **37**, 4227–4237 (2012)
28. Wang, P., Wang, A., Zhang, H., Ding, B., Hu, Z.: Hydrogenation characteristics of Mg–TiO_2 (rutile) composite. J. Alloy. Compd. **313**, 218–223 (2000)
29. Jung, K.S., Kim, D.H., Lee, E.Y., Lee, K.S.: Hydrogen sorption of magnesium hydride doped with nano-sized TiO 2. Catal. Today **120**, 270–275 (2007)
30. Wang, P., Zhang, H., Ding, B., Hu, Z.: Direct hydrogenation of Mg and decomposition behavior of the hydride formed. J. Alloy. Compd. **313**, 209–213 (2000)
31. Gattia, D.M., Di Girolamo, G., Montone, A.: Microstructure and kinetics evolution in MgH_2–TiO_2 pellets after hydrogen cycling. J. Alloy. Compd. **615**, S689–S692 (2014)
32. Croston, D.L.: The Effect of Metal Oxide Additives on the Hydrogen Sorption Behaviour of Magnesium Hydride. Doctoral dissertation, University of Nottingham (2007)
33. Hanada, N., Ichikawa, T., Fujii, H.: Catalytic effect of nanoparticle 3d-transition metals on hydrogen storage properties in magnesium hydride MgH_2 prepared by mechanical milling. J. Phys. Chem. B **109**, 7188–7194 (2005)
34. Khrussanova, M., Terzieva, M., Peshev, P., Konstanchuk, I., Ivanov, E.: Hydriding of mechanically alloyed mixtures of magnesium with MnO_2, Fe_2O_3 and NiO. Mater. Res. Bull. **26**, 561–567 (1991)
35. Cabo, M., Garroni, S., Pellicer, E., Milanese, C., Girella, A., Marini, A., et al.: Hydrogen sorption performance of MgH_2 doped with mesoporous nickel-and cobalt-based oxides. Int. J. Hydrog. Energy **36**, 5400–5410 (2011)
36. Simchi, H., Kaflou, A., Simchi, A.: Synergetic effect of Ni and Nb_2O_5 on dehydrogenation properties of nanostructured MgH_2 synthesized by high-energy mechanical alloying. Int. J. Hydrog. Energy **34**, 7724–7730 (2009)
37. Williamson, G., Hall, W.: X-ray line broadening from filed aluminium and wolfram. Acta Metall. **1**, 22–31 (1953)
38. Hosseini-Gourajoubi, F., Pourabdoli, M., Uner, D., Raygan, S.: Effect of process control agents on synthesizing nano-structured 2 Mg–9Ni–Y catalyst by mechanical milling and its catalytic effect on desorption capacity of MgH_2. Adv. Powder Technol. **26**, 448–453 (2015)
39. Shahi, R.R., Bhatnagar, A., Pandey, S.K., Dixit, V., Srivastava, O.: Effects of Ti-based catalysts and synergistic effect of SWCNTs-TiF_3 on hydrogen uptake and release from MgH_2. Int. J. Hydrog. Energy **39**, 14255–14261 (2014)
40. Huot, J., Liang, G., Boily, S., Van Neste, A., Schulz, R.: Structural study and hydrogen sorption kinetics of ball-milled magnesium hydride. J. Alloy. Compd. **293**, 495–500 (1999)
41. Varin, R., Czujko, T., Wronski, Z.: Particle size, grain size and γ-MgH_2 effects on the desorption properties of nanocrystalline commercial magnesium hydride processed by controlled mechanical milling. Nanotechnology **17**, 3856 (2006)
42. Walker, G.: Solid-State Hydrogen Storage: Materials And Chemistry. Elsevier, Woodhead Publishing Limited, Cambridge, England (2008)
43. Reule, H., Hirscher, M., Weißhardt, A., Kronmüller, H.: Hydrogen desorption properties of mechanically alloyed MgH_2 composite materials. J. Alloy. Compd. **305**, 246–252 (2000)
44. Ranjbar, A.: Effect of catalysts on hydrogen storage properties of MgH_2. Doctoral dissertation, Faculty of Engineering, University of Wollongong (2010)
45. Au, Y.S., Obbink, M.K., Srinivasan, S., Magusin, P.C., De Jong, K.P., De Jongh, P.E.: The size dependence of hydrogen mobility and sorption kinetics for carbon-supported MgH2 particles. Adv. Funct. Mater. **24**, 3604–3611 (2014)
46. Liu, G., Wang, K., Li, J., Wang, Y., Yuan, H.: Enhancement of hydrogen desorption in magnesium hydride catalyzed by graphene nanosheets supported Ni-CeO x hybrid nanocatalyst. Int. J. Hydrog. Energy **41**(25), 10786–10794 (2016)
47. ChitsazKhoyi, L., Raygan, S., Pourabdoli, M.: Effect of synthesized $MgNi_4Y$ catalyst on hydrogen desorption properties of milled MgH_2. Metall. Mater. Trans. E **2**, 27–32 (2015)
48. Pourabdoli, M., Raygan, S., Abdizadeh, H., Uner, D.: A comparative study for synthesis methods of nano-structured (9Ni–2 Mg–Y) alloy catalysts and effect of the produced alloy on hydrogen desorption properties of MgH_2. Int. J. Hydrog. Energy **38**, 16090–16097 (2013)
49. Mitchell, P.C., Ramirez-Cuesta, A.J., Parker, S.F., Tomkinson, J., Thompsett, D.: Hydrogen spillover on carbon-supported metal catalysts studied by inelastic neutron scattering. Surface vibrational states and hydrogen riding modes. J. Phys. Chem. B **107**, 6838–6845 (2003)
50. Wang, Y., Wu, S.W., Yu, H., Gong, N.N., Cao, Z.Q., Zhang, K.: Hydrogen desorption/absorption kinetics of MgH_2 catalyzed with TiO_2. Adv. Mater. Res. **986**, 88–91 (2014)
51. Wang, Y., Zhang, Q., Wang, Y., Jiao, L., Yuan, H.: Catalytic effects of different Ti-based materials on dehydrogenation performances of MgH_2. J. Alloy. Compd. **645**, S509–S512 (2015)